Depth dependence of itinerant character in Mn-substituted $Sr_3Ru_2O_7$

Depth dependence of itinerant character
in Mn-substituted $Sr_3Ru_2O_7$

G Panaccione[1,9]**, U Manju**[2]**, F Offi**[3]**, E Annese**[1]**, I Vobornik**[1]**,
P Torelli[1]**, Z H Zhu**[4]**, M A Hossain**[4]**, L Simonelli**[5]**, A Fondacaro**[5]**,
P Lacovig[6]**, A Guarino**[7]**, Y Yoshida**[8]**, G A Sawatzky**[4] **and
A Damascelli**[4]

[1] Istituto Officina dei Materiali CNR, TASC, Area Science Park, SS 14,
Km 163.5, I-34149 Trieste, Italy
[2] The Abdus Salaam International Center for Theoretical Physics (ICTP),
PO Box 586, I-34014 Trieste, Italy
[3] CNISM and Dipartimento di Fisica Università Roma Tre, via della Vasca
Navale 84, I-00146 Rome, Italy
[4] Department of Physics and Astronomy, University of British Columbia,
Vancouver, British Columbia, V6T 1Z1, Canada
[5] European Synchrotron Radiation Facility, BP 220, F-38042 Grenoble, France
[6] Sincrotrone Trieste S.C.p.A., Area Science Park, SS 14, Km 163.5,
I-34012 Trieste, Italy
[7] CNR-SPIN UOS Salerno and Dipartimento di Fisica "E. R. Caianiello",
Università di Salerno, 84084 Fisciano (SA), Italy
[8] Natonal Institute of Advanced Industrial Science and Technology (AIST),
Tsukuba 305-8568, Japan
E-mail: giancarlo.panaccione@elettra.trieste.it

Abstract. We present a core-level photoemission study of $Sr_3(Ru_{1-x}Mn_x)_2O_7$, in which we monitor the evolution of the Ru-*3d* fine structure versus Mn substitution and probing depth. In both Ru-*3d$_{3/2}$* and -*3d$_{5/2}$* core levels, we observe a clear suppression of the metallic features, i.e. the screened peaks, implying a sharp transition from itinerant to localized character already at low Mn concentrations. A comparison of soft and hard x-ray photoemission, which enables tunable depth sensitivity, reveals that the degree of localized/metallic character for Ru at the surface is different from that in the bulk.

[9] Author to whom any correspondence should be addressed.

IOP Institute of Physics Φ DEUTSCHE PHYSIKALISCHE GESELLSCHAFT

Contents

1. Introduction

Inducing changes in carrier density by chemical doping is one of the most commonly used techniques for tailoring novel properties in a variety of materials, including strongly correlated electron systems. Transition metal oxides (TMO) are paradigmatic in this sense: they often display many different electronic phases that are quite close in energy. A comprehensive description of TMO can be achieved only by disentangling such different, yet comparable, energy scales. Research on the RuO family $(Sr, Ca)_{n+1}Ru_nO_{3n+1}$ has recently suggested a conceptually different approach, based on the substitution of *4d* Ru with a *3d* transition metal impurity. A central feature of the physics of Ru oxides is the spatial extension of *4d* orbitals: the properties of ruthenates are extremely sensitive to the orbital degrees of freedom, resulting in almost equal chances of displaying itinerant or localized behavior. The substitution of Ru-*4d* with more localized *3d* metal atoms will strongly influence the orbital population, possibly resulting in orbital-induced novel properties. An example of this approach is the use of chromium (Cr^{4+}) in $SrRu_{1-x}Cr_xO_3$ and $CaRu_{1-x}Cr_xO_3$ to stabilize itinerant ferromagnetism from the normal paramagnetic state [1, 2]. More recently, a 5% Ru–Mn substitution in the bilayer compound $Sr_3Ru_2O_7$ was proved to change the ground state from a paramagnetic metal to an unconventional, possibly Mott-like antiferromagnetic insulator [3, 4]. The interplay between the extended, yet anisotropic Ru-*4d* and O-*2p* bonds and the localized Mn-*3d* impurity states was shown to be responsible for a crystal-field level inversion, with Mn not exhibiting the expected Mn^{4+} valence but rather acting as an Mn^{3+} acceptor [5], a behavior bearing interesting similarities to the dilute magnetic semiconductor Mn-doped GaAs.

Unravelling what ultimately drives the electronic and magnetic properties of the $Sr_3(Ru_{1-x}Mn_x)_2O_7$-doped system is strictly linked to a direct measure of the electronic charge distribution over Ru- and O-ligand orbitals. Since it is well known that electron correlations in TMO, and in particular in ruthenates, are strongly influenced by the surface environment (cleavage plane, electronic/structural reconstruction and defects) [6–9], a comparison with reliable bulk-sensitive probes is mandatory. Photoemission spectroscopy (PES) possesses all of the characteristics necessary in elucidating the aforementioned rich physics. In particular, core-level PES probes the different electronic screening channels via the energy location and relative intensity ratio of specific peaks, in a chemically selective way. This possibility is confirmed by recent experimental results in [10], where a systematic study of doping and dimensionality effects in the core level of various ruthenates was carried out at fixed photon energy (Al K-α radiation, 1486.7 eV).

In this paper, we report a study of the Ru-*3d* core-level fine structure versus Mn concentration in $Sr_3(Ru_{1-x}Mn_x)_2O_7$ by soft x-ray PES and hard x-ray PES (HAXPES), hence

with tunable depth sensitivity. The choice of focusing on the Ru-*3d* core levels, as opposed, for instance, to the Mn-*2p* spectra, is dictated by their sharper nature, which allows tracking more precisely the fine satellite structure (we measured Mn-*2p* spectra by HAXPES, obtaining results analogous to those reported in [10]; no extra satellites were observed). Already at low energy, an Mn-induced suppression of the screened metallic features is observed in both Ru-$3d_{3/2}$ and Ru-$3d_{5/2}$, implying a transition from itinerant to localized character, in analogy to the reported metal-to-insulator transition (MIT) [3, 5]. HAXPES data confirm the change upon Mn substitution, with a clear indication of a stronger electronic localization at the surface than in the bulk. Our results suggest a way to control, in the same material, the metallicity of the surface–interface region versus the bulk one by exploiting the highly sensitive response of conducting perovskites to impurities.

2. Experimental methods

High-quality single crystals of $Sr_3(Ru_{1-x}Mn_x)_2O_7$, with $x = 0$, 0.05 and 0.2, were grown by the floating zone technique. PES measurements were carried out after fracturing the samples in UHV using two experimental setups: an APE beamline for low-energy PES (Elettra, $h\nu = 455$ eV, base pressure 1×10^{-10} mbar) [11] and a VOLPE spectrometer for HAXPES (beamline ID16 at ESRF, $h\nu = 7595$ eV, base pressure 6×10^{-10} mbar) [12]. The spot size in the normal emission geometry was $50 \times 120\,\mu m^2$ in both cases, and the overall beamline-analyzer energy resolution was set to 200 meV (APE) and 350 meV (VOLPE). The Fermi energy and overall energy resolutions were estimated by measuring a polycrystalline Au foil in thermal and electric contact with the samples. Identical results were obtained consistently on several cleaved samples. The cleanliness of the surface was checked by monitoring the *C-1s* and *O-1s* spectra. With soft x-ray, a new cleave was needed every ∼4 h; instead, no traces of contamination were observed, over 2 days and at any temperature, in HAXPES measurements.

3. Results and discussion

Surface-sensitive ($h\nu = 455$ eV) Ru-*3d* core-level spectra from $Sr_3(Ru_{1-x}Mn_x)_2O_7$ are presented in figures 1 and 2. In figure 1, we identify the Sr-$3p_{1/2}$ peak at about 279 eV of binding energy (BE) and the Ru spin–orbit split doublet $3d_{5/2}$ and $3d_{3/2}$ in the 280–295 eV BE range. Both Ru-$3d_{5/2}$ and -$3d_{3/2}$ spectra display multiple components, which have already been observed in the ruthenates; it is generally agreed that the low BE features are not induced by surface-related chemical states, and their spectral weight increases when the system enters a metallic regime [10], [13–16]. More specifically, each spin–orbit partner is comprised of a low BE peak, corresponding to the relaxed lowest-energy core-hole state and referred to as the screened state, and a broader higher BE structure associated with the unscreened core-hole state. The remarkable sensitivity to surface environment is observed via the evolution versus time of the Ru-*3d* spectral lineshape in pure $Sr_3Ru_2O_7$. While on freshly cleaved surfaces the various spectral components are well separated, surface contamination strongly changes the lineshapes, as evidenced by (i) intense *C-1s* structures at ∼285 eV BE; (ii) a suppression of the screened peaks; and (iii) the appearance of a shoulder at ∼288 eV of BE. We emphasize that the average photoelectron mean-free path at this photon energy ranges from 4 to 8 Å [17].

In figure 2, we present the evolution of the Ru-*3d* spectrum as a function of Mn substitution *x*.
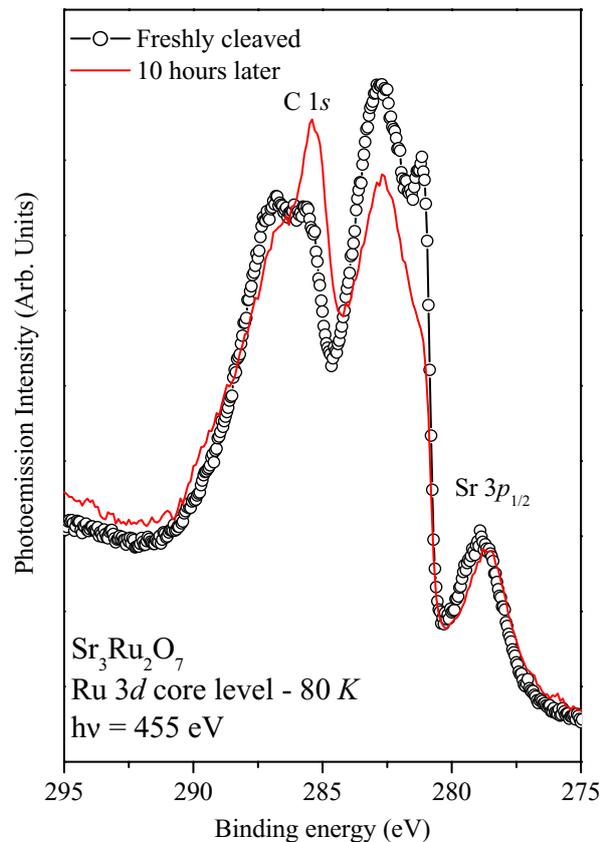
Figure 1. Evolution versus time of the Ru-*3d* core-level spectra from $Sr_3Ru_2O_7$ collected at $h\nu = 455$ eV ($T = 80$ K) on a freshly cleaved surface and after 10 h. In the latter case, the intense *C-1s* contribution located at ~ 286 eV BE is clearly visible, while the screened peaks on the low BE side of both Ru-*3d$_{3/2}$* and -*3d$_{5/2}$* lines are almost absent.

The intense screened features, for both Ru-*3d$_{5/2}$* and Ru-*3d$_{3/2}$*, are severely suppressed already at $x = 5\%$ and reduce to only a weak shoulder for $x = 20\%$; an energy shift for the screened features of up to 100 meV for 20% Mn substitution is observed, as in [10]. In addition, the difference spectra at the bottom of figure 2 highlight the redistribution of spectral weight upon Mn substitution; their lineshape reveals their fine structure (with sizeable intensities around 281.3 and 285.5 eV BE), and clear shoulders on the high BE side of each spin–orbit partner (centered at 287 and 283 eV BE). These broad shoulders can be ascribed to multiplet structure, which becomes more prominent upon Mn substitution, possibly suggesting the evolution from itinerant to localized character. It is interesting to note that both 5 and 20% Mn-doped spectra display close similarities to Ru-*3d* core-level results from Ca_2RuO_4, a pure antiferromagnetic insulator [18]. This suggests that the suppression of the screened features is compatible with metal–insulator transition induced by Mn substitution in $Sr_3(Ru_{1-x}Mn_x)_2O_7$.

Regarding the underlying driving mechanism of the transition, a purely electronic scenario was proposed based on the detection by REXS of an associated magnetic superstructure [4] and on the comparison of linear dichroism XAS data and density functional theory calculations [5]. While the evolution of the screened states in the present XPS study is compatible with the
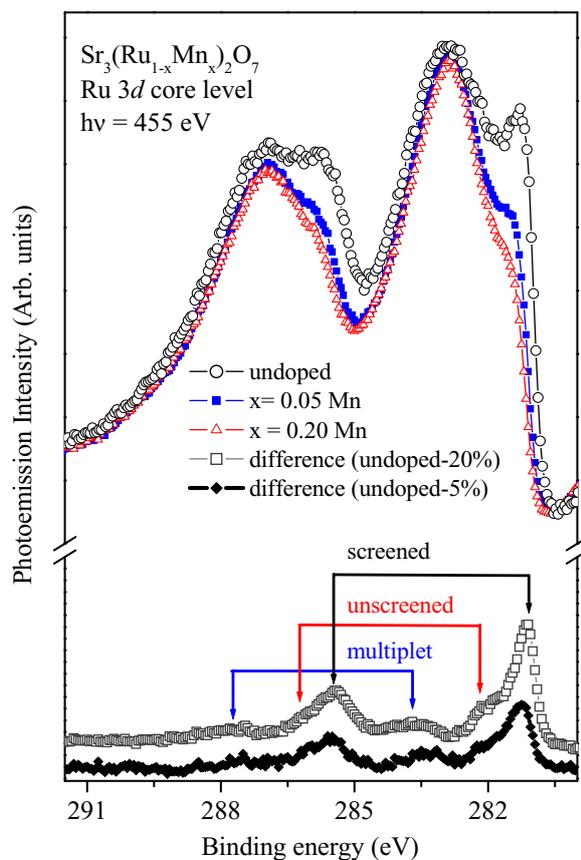
Figure 2. Ru-*3d* core-level spectra collected at $h\nu = 455\,\text{eV}$ ($T = 80\,\text{K}$) on $Sr_3(Ru_{1-x}Mn_x)_2O_7$ for $x = 0$, 0.05 and 0.2. The spectra have been normalized at the Sr-$3p_{1/2}$ peak (279 eV BE, see figure 1). A clear suppression of the screened features located at the low BE side of both spin–orbit partners is observed upon Mn doping. In the bottom of the figure, the difference spectra, obtained after subtraction of the Mn-doped spectrum from the undoped one ((Undoped−20%) and (Undoped−5%)), are presented, highlighting the change in spectral shape. The three bars indicate the energy position of the three sets of doublets corresponding to the main intensities (screened, unscreened and multiplet). The three doublets have been used to fit the experimental spectra in figure 4. A shift in the energy position upon Mn doping is observed for the peaks as well as for the multiplet contribution on the high BE side

proposed electronic-driven transition induced by Mn impurities playing the role of Mn^{3+} acceptors [4, 5], PES does not allow determining the precise location of additional holes in the Ru oxide host [10]. One could expect that two components should be observed in the Ru core-level spectra, associated with Ru^{4+} and Ru^{5+}, respectively. For 5 to 20% Mn substitution, at most 5 to 20% Ru atoms would be in a 5+ oxidation state, i.e. a very unfavorable case for measuring different contributions in the broad Ru-*3d* structure, where at least 80% of the intensity is of Ru^{4+} character. Moreover, the induced holes would most likely be in delocalized states involving oxygen ligands, which would make their detection in XPS even less likely. One might speculate
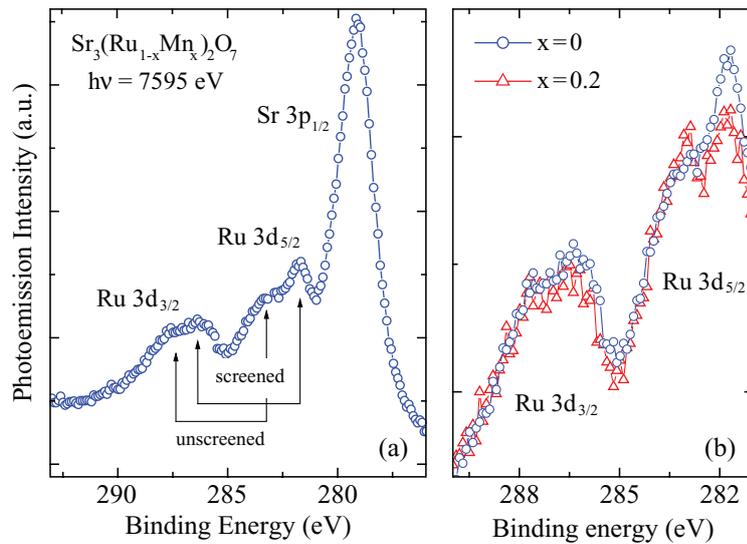
Figure 3. Ru-*3d* core-level spectra acquired at $h\nu = 7595$ eV ($T = 20$ K) on $Sr_3(Ru_{1-x}Mn_x)_2O_7$ for $x = 0$ and 0.2. (a) Spectral region including the Sr-*3p$_{1/2}$* core level; the Sr-*3p* intensity is higher than the Ru-*3d* one, due to the photoionization cross section increase in the HAXPES regime. (b) Enlarged view of the Ru-*3d* energy range; for clarity, the spectra have been normalized to the Sr-*3p$_{1/2}$* intensity. A reversed peak/height ratio between screened and unscreened features, for both *3d$_{5/2}$* and *3d$_{3/2}$*, is observed.

that the lack of detection of an Ru^{5+} oxidation state, in ours and Guo *et al*'s [10] XPS results, supports a scenario where Mn-induced holes are indeed delocalized.

The evolution of MIT described in [3] indicates a progressive increase in resistivity versus Mn doping, e.g. resistivity increases by a factor of 10 between pure $Sr_3Ru_2O_7$ and the 5% Mn-doped one. The gradual suppression of electrical conductivity upon Mn doping, measured by a bulk property such as resistivity, is reflected in the decrease in screening features in photoemission. It is important to remember, however, that photoemission, with a varying degree of probing depth, is a surface-sensitive technique. Surface-sensitive spectra in figure 2 display a particularly pronounced decrease of the screened intensity already at 5% Mn doping. The 5% spectrum is indeed closer to the 20% spectrum than one might expect on the basis of the bulk properties, suggesting that MIT is more pronounced at the surface than in the bulk. The residual intensity observed in the screened features of figure 2 upon Mn doping can be ascribed to the gradual evolution from metallic- to insulator-like character. Although the evolution of the PES intensity clearly identifies the trend, a quantitative analysis is impossible, in particular because the studied system is not a true large-gap insulator.

The extreme sensitivity of the screened features—and hence of the available screening channels—to the local environment calls for a more accurate determination of the metallic-insulating character upon Mn substitution. To this end, in figure 3 we present HAXPES results that guarantee a bulk sensitivity of ~8 nm [19]. The relative intensity of Sr and Ru peaks is significantly different with respect to the soft x-ray data (figures 1 and 3(a)), which stems from the change in *p/d* cross-section ratio when passing from soft x-ray PES to HAXPES [19, 20]. Zooming on the Ru-*3d* region (figure 3(b)), screened peaks are again observed in pure $Sr_3Ru_2O_7$

together with a clear decrease of their intensity upon Mn substitution. Although the evolution as a function of Mn concentration is confirmed, the relative peak/height ratio between unscreened and screened features is reversed with respect to the surface-sensitive results. On the basis of the enhanced probing depth of HAXPES [17, 19], the intensity increase of screened peaks observed on *3d*-based TMO in the hard x-ray regime has been recently interpreted as a fingerprint of different screening mechanisms between surface and volume [21–25]. HAXPES results in vanadates across the metal–insulator transition also confirm the relationship between low BE features and metallicity [26].

We stress that our data cannot provide direct evidence for the exclusive electronic-driven picture and we have only a compatible scenario with the one described by Hossain *et al* [4]. While we can directly show by soft and hard x-ray photoemission, and the relative intensity of screened peaks, that the surface is more correlated than the bulk, we cannot address directly the role and interplay of other degrees of freedom, such as charge, spin and lattice.

To better disentangle screened and poorly screened features and also to identify any additional components, we performed a spectral decomposition by fitting routines. Each peak was represented by a symmetric function generated by a Lorentzian lineshape convoluted with a Gaussian. The Lorentzian function represents the lifetime broadening effect, while the Gaussian accounts for all other broadenings including energy resolution (350 meV for HAXPES and 200 meV for soft x-ray). The results on these spectral decompositions are presented in figure 4 and the corresponding parameters are summarized in table 1. The open circles in figure 4 show the experimental spectra and the solid line shows the fitting. The spectra recorded at 455 eV photon energy could be best fitted using such a function with three sets of doublets (screened, unscreened and multiplet peaks), where the intensity ratio between the spin–orbit split components has been fixed at 1.5, as determined by the degeneracy ratio. The multiplet structures appearing on the higher BE side, for both $3d_{5/2}$ and $3d_{3/2}$ components, have been modeled with Gaussian intensities and constrained to the energy position of the structures appearing in figure 2. The fitting procedure confirms the reduction of such a multiplet contribution upon Mn substitution. For the bulk-sensitive spectra recorded at $h\nu = 7595$ eV, the best fit is obtained with two sets of doublets only; in this case, adding a multiplet contribution does not increase significantly the quality of the fit. This is partly due to the residual intensity at high BE arising from the Sr-*3p* core level, which limits the analysis of fine details in the HAXPES spectra. The integrated intensity ratio between screened and unscreened peaks is summarized in table 1. At each photon energy, the values are identical within the error bars, for both $3d_{5/2}$ and $3d_{3/2}$ components, confirming that (i) no extra intensity (hence a different ratio for different spin–orbit partners) arising from contamination is found, knowing that C-1s signal overlaps with $3d_{3/2}$; (ii) the evolution of the metallic/insulating behavior upon Mn substitution is different in the cases of the bulk and the surface; (iii) regarding the surface-sensitive data, the results of the fit indicate not only a shift to higher BE of the screened peaks but also a shift, in the same direction, of the unscreened contributions. All of these findings point again to an important modification of the surface electronic structure compared to the bulk one.

The presence and evolution of screened and unscreened features in the *4d* PES spectra from ruthenates have been described in terms of a Mott–Hubbard picture within a dynamical mean field theory (DMFT) approach [27]; cluster calculations of Ru-*3d* in Sr_2RuO_4 suggest that the energy separation between screened and unscreened peaks is reminiscent of the Coulomb interaction between Ru-*3d* and -*4d* holes, and comparable with the Ru-*4d*-t_{2g} bandwidth W [28]. In particular, smaller U_{dd} values correspond to higher screened intensity; thus, the observed
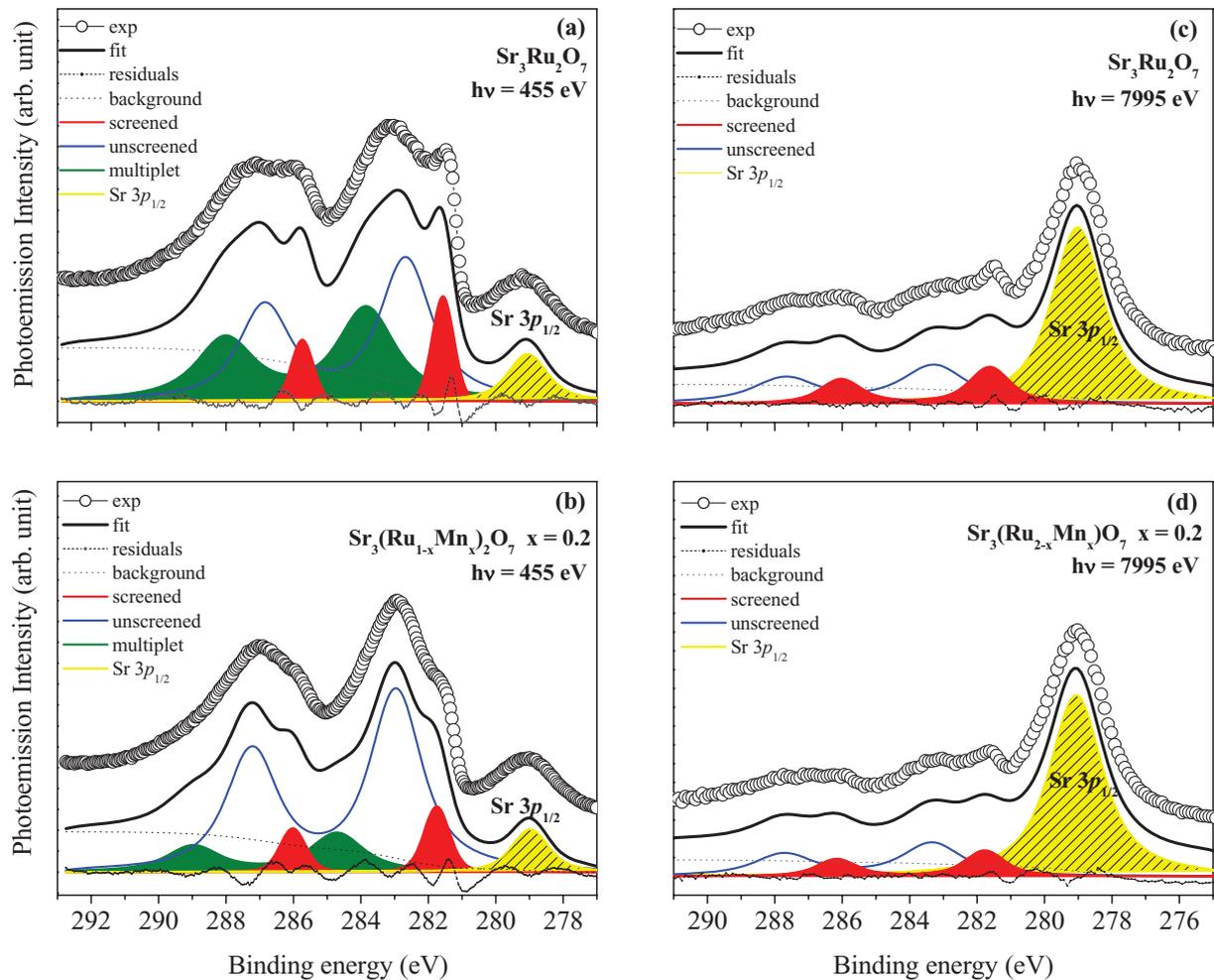
Figure 4. Fit of the Ru-*3d* spectra measured at $h\nu = 455$ (a, b) and 7595 eV (c, d). The Gaussian instrumental resolution broadening is $\sim$350 meV at 7595 eV and $\sim$200 meV at 455 eV; backgrounds proportional to the integrated intensity and residual intensity are also included (black dotted curve and dotted curve, respectively). For the Ru-*3d* doublets (blue curves, red curves and green curves) a $\sim$4 eV spin–orbit splitting and a 1 : 1.5 statistical intensity ratio are imposed. Energy positions of peaks are normalized to the Sr $3p_{1/2}$ peak (yellow curves).

difference between surface- and bulk-sensitive PES spectra suggests a stronger localization in the surface and subsurface region, as possibly due to the reduced coordination or surface relaxation. The interpretation in terms of final-state screening properties, supported by both experimental and theoretical considerations, also suggests that the linewidth of the screened peak bears a degree of proportionality to the Ru bandwidth W [27–29]; due to the increase in electron localization in passing from volume to surface, one would expect a line narrowing in surface-sensitive PES, reflecting the progressive reduction of W. This argument appears to be corroborated by the linewidth fit results for the screened peak in HAXPES and soft x-ray PES. Although the experimental energy resolution is similar for the different kinetic energy ranges, the Lorentzian contribution of the screened features is sharper in the soft x-ray (full-width

Table 1. Parameters of the Ru-$3d$ core-level spectral analysis. I_S/I_U refers to the integrated intensity ratio of the Ru-$3d_{5/2}$ screened (S) and unscreened (U) peaks; within uncertainties, identical values are found for the Ru-$3d_{3/2}$ features.

$h\nu$ (eV)	Compound	I_S/I_U
455	$Sr_3Ru_2O_7$	0.23
455	$Sr_3(Ru_{1.6}Mn_{0.4})O_7$	0.16
7595	$Sr_3Ru_2O_7$	0.89
7595	$Sr_3(Ru_{1.6}Mn_{0.4})O_7$	0.63

at half-maximum (FWHM) $\sim 300\,meV$) than in the HAXPES regime (FWHM $\sim 600\,meV$). Note, however, that a conclusive unambiguous statement on this latter point is prevented by the broad nature of the experimental features, which renders the value of this observation purely qualitative.

4. Conclusions

In conclusion, the $Sr_3(Ru_{1-x}Mn_x)_2O_7$ metal–insulator transition has been studied by variable probing depth PES. The measured evolution of the Ru-$3d$ core-level signals provides evidence for a progressive increase of electron correlations, not only upon doping but also from the bulk to the surface. The reduction of metallic-like screening channels, which is more pronounced in the vicinity of the surface, might also play a role at interfaces, leading to potentially new physical properties.

Acknowledgments

References

[1] Williams A J, Gillies A, Attfield J P, Martínez-Lope M J, Alonso J A, Heymann G and Huppertz H 2006 *Phys. Rev.* B **73** 104409
[2] Durairaj V, Chikara S, Lin X N, Douglass A, Cao G, Schlottmann P, Choi E S and Guertin R P 2006 *Phys. Rev.* B **73** 214414
[3] Mathieu R *et al* 2005 *Phys. Rev.* B **72** 092404
[4] Hossain M A 2009 (arXiv:0906.0035)
[5] Hossain M A *et al* 2008 *Phys. Rev. Lett.* **101** 016404
[6] Matzdorf R, Fang Z, Ismail, Zhang J, Kimura T, Tokura Y, Terakura K and Plummer E W 2000 *Science* **289** 746
[7] Damascelli A *et al* 2000 *Phys. Rev. Lett.* **85** 5194
[8] Sekiyama A *et al* 2004 *Phys. Rev.* B **70** 060506

[9] Pennec Y, Ingle N J C, Elfimov I S, Varene E, Maeno Y, Damascelli A and Barth J V 2008 *Phys. Rev. Lett.* **101** 216103

[10] Guo H *et al* 2010 *Phys. Rev.* B **81** 155121

[11] Panaccione G *et al* 2009 *Rev. Sci. Instrum.* **80** 043105

[12] Torelli P *et al* 2005 *Rev. Sci. Instrum.* **76** 023909

[13] Schmidt M, Cummins T R, Bürk M, Lu D H, Nücker N, Schuppler S and Lichtenberg F 1996 *Phys. Rev.* B **53** R14761

[14] Hyeong-Do, K, Han-Jin N, Kim H K and Oh S J 2004 *Phys. Rev. Lett.* **93** 126404

[15] Sekiyama A *et al* 2004 *Phys. Rev. Lett.* **93** 156402

[16] Takizawa M *et al* 2005 *Phys. Rev.* B **72** 060404

[17] NIST US 2000 *NIST Electron Inelastic-Mean-Free-Path Database, Version 1.1*

[18] Noh H J 2003 *PhD Thesis* Seoul National University

[19] Sacchi M *et al* 2005 *Phys. Rev.* B **71** 155117

[20] Yeh J J and Lindau I 1985 *At. Data Nucl. Data Tables* **32** 1

[21] Panaccione G *et al* 2005 *J. Phys.: Condens. Matter* **17** 2671

[22] Taguchi M *et al* 2005 *Phys. Rev. Lett.* **95** 177002

[23] Taguchi M *et al* 2005 *Phys. Rev.* B **71** 155102

[24] Horiba K *et al* 2004 *Phys. Rev. Lett.* **93** 236401

[25] van Veenendal M A 2006 *Phys. Rev.* B **74** 085118

[26] Panaccione G *et al* 2006 *Phys. Rev. Lett.* **97** 116401

[27] Okada K 2002 *Surf. Rev. Lett.* **9** 1023

[28] Kotani A and Toyazawa Y 1974 *J. Phys. Soc. Japan* **37** 912

[29] Cox P A, Egdell R G, Goodenough J B, Hamnett A and Naish C C 1983 *J. Phys. C: Solid State Phys.* **16** 6221